J. theor. Biol. (1998) **190,** 135–146

Hematopoietic Model with Moving Boundary Condition and State Dependent Delay: Applications in Erythropoiesis

JOSEPH M. MAHAFFY*,‖, JACQUES BÉLAIR†,‡,¶ AND MICHAEL C. MACKEY§,¶

* *Department of Mathematical Sciences, San Diego State University, San Diego, CA* 92182, *U.S.A.*;
† *Département de mathématiques et de statistique and*
‡ *Centre de recherches mathématiques, Université de Montréal, Montreal, Quebec, Canada*;
§ *Department of Physiology and*
¶ *Centre for Nonlinear Dynamics in Physiology and Medicine, McGill University, Montreal, Quebec H3G 1Y6, Canada*

(*Received on* 28 *February* 1997, *Accepted in revised form on* 19 *August* 1997)

An age-structured model for erythropoiesis is extended to include the active destruction of the oldest mature cells and possible control by apoptosis. The former condition, which is applicable to other population models where the predator satiates, becomes a constant flux boundary condition and results in a moving boundary condition. The method of characteristics reduces the age-structured model to a system of threshold type differential delay equations. Under certain assumptions, this model can be reduced to a system of delay differential equations with a state dependent delay in an uncoupled differential equation for the moving boundary condition. Analysis of the characteristic equation for the linearized model demonstrates the existence of a Hopf bifurcation when the destruction rate of erythrocytes is modified. The parameters in the system are estimated from experimental data, and the model is simulated for a normal human subject following a loss of blood typical of a blood donation. Numerical studies for a rabbit with an induced auto-immune hemolytic anemia are performed and compared with experimental data.

1. Introduction

Age-structured models provide a means of understanding the regulation of hematopoiesis. Poor regulation of this physiological system appears to underlie several hematological disorders that display oscillatory counts in their cell numbers (Milton & Mackey, 1989; Morley, 1970), i.e. cyclic neutropenia (also known as periodic hematopoiesis) (Dale & Hammond, 1988; Jones & Lange, 1983; Lange, 1983; Wright *et al*., 1981), cyclic thrombocytopenia (Bernard & Caen, 1962; Brey *et al*., 1969; Caen *et al*., 1964; Cohen & Cooney, 1974; Demmer, 1920; Engstrom *et al*., 1966; Goldsmith & Fono, 1972; Lewis, 1974; Skoog *et al*., 1957; Wasatjerna, 1967; Wilkinson & Firkin, 1966), cyclic eosinophilic myositis and hyper-immunolobulin E syndrome (Symmans *et al*., 1986), and the periodic variants of chronic myelogenous leukemia (Chikkappa *et al*., 1976; Delobel *et al*., 1973; Gatti *et al*., 1973; Kennedy, 1970; Morley *et al*., 1967; Nowell *et al*., 1988; Shadduck *et al*., 1972; Mastrangelo *et al*., 1974, 1976; Rodriguez & Lutcher, 1976; Umemura *et al*., 1986; Yamauchi & Ide, 1992) and autoimmune hemolytic anemia (Gordon & Varadi, 1962; Orr *et al*., 1968; Ranlov & Videbaek, 1963).

It has long been suspected that periodic hematological diseases arise because of abnormalities in the feedback mechanisms which regulate blood cell number (Dunn, 1983; Kazarinoff & van den Driessche, 1979; King-Smith & Morley, 1970; Kirk

‖ Author to whom correspondence should be addressed.
E-mail: mahaffy@saturn.SDSU.edu

0022–5193/98/020135 + 12 $25.00/0/jt970537

et al., 1968; Mackey, 1978, 1979a,b, 1996; Mackey & Milton, 1990; Morley, 1979; von Schulthess & Mazer, 1982; Wazewska-Czyzewska, 1984; Wheldon *et al*., 1974; Wheldon, 1975; Wichmann & Loeffler, 1988). Previously, we developed an age-structured model for erythropoiesis whose bifurcation analysis agreed surprisingly well with experimental observations in an induced autoimmune hemolytic anemia (Bélair *et al*., 1995). However, this model was less satisfactory in predicting the response of a normal patient to a blood loss such as a blood donation. In this paper we expand this previous model (Bélair *et al*., 1995) to account for the active degradation of older cells and to include the possibility of significant preprogrammed cellular death (apoptosis).

The idea that older cells are actively degraded has several applications to the study of population dynamics. Erythrocytes age primarily by damage to their cell membrane as they pass through the capillaries (Erslev & Beutler, 1995). Since erythrocytes have no nucleus to produce proteins that effect repair of the cell membrane, the membrane slowly loses pliability and the cells can no longer efficiently deliver O_2 to the tissues. The immune system recognizes this membrane breakdown and tags the membrane with special markers. These markers then signal macrophages or white blood cells to actively degrade or phagocytize the oldest erythrocytes after a period of time that is about 120 days in humans.

In an ecological context, many populations have older individuals actively weeded out by predators. The predators, however, generally have a finite appetite and satiate. Thus, for example, an overabundance of hares will not result in incidence of obesity in lynx populations, but rather in a self-regulation of calorie intake on their part [possible predator behaviors in the presence of an oversupply of prey have been discussed recently (Crichton, 1995)].

For erythrocytes, if one assumes either a finite source of markers or a fixed number of macrophages, then there is a constant flux of the oldest erythrocytes dying. This moving boundary condition is incorporated in this paper and represents a significant improvement to our previous model (Bélair *et al*., 1995).

Apoptosis (Evan *et al*., 1985; Koury, 1992; Park, 1996; Yuan, 1995) is a programmed cell death that is probably determined by the genetic code of the cell. As an example, in erythropoiesis it appears that many burst-forming units of the erythroid line (BFU-E) begin their proliferative phase with genetic instructions that kill the cell unless the signal is interrupted by sufficient binding of erythropoietic (Epo) to the cell membrane (Adamson, 1995). This death generally occurs when the cells enter the next stage of development, colony forming units or CFU-Es, and provides a control that prevents the production of too many erythrocytes. Apoptosis is incorporated in our general model, but has little effect on the analysis of the simplified model with delay differential equations.

In the next section we present our age-structured model and show how it reduces to a threshold delay system. In Section 3, we show with several simplifying assumptions that the model further reduces to a system of delay differential equations with a state-dependent delay in an uncoupled differential equation for the moving endpoint. A bifurcation analysis is performed in Section 4, and numerical studies in Section 5 examine two responses of erythropoiesis: one following a blood donation in humans and the second a hemolytic-induced anemia in rabbits. Comparisons are made to an earlier study (Bélair *et al*., 1995), where the age of the mature erythrocyte was assumed to be fixed. The paper concludes with a brief discussion in Section 6.

2. The Age-structured model with Constant Flux

In this section we present an age-structured model for hematopoiesis that includes apoptosis and active degradation of the oldest mature cells. This extended model is based on an earlier model of Bélair *et al*. (1995). For clarity, our model is described for erythropoiesis, but it is sufficiently general to characterize other hematopoietic lines. The active degradation of the oldest mature cells extends easily to other models with predation.

The precursor cells begin from a pool of BFU-Es that have differentiated into a self-sustaining population which eventually leads to the production of mature erythrocytes. At some point the BFU-Es further differentiate and start down a proliferative path that can ultimately produce erythrocytes. Early in this proliferative phase of development the hormone Epo, along with other hormones, affects the number of BFU-Es that become erythrocytes, though the full details of the mechanism remain unknown. Increases in the concentration of Epo may increase the number of BFU-Es recruited to mature into erythrocytes. Alternatively, there may be a relatively constant supply of committed BFU-Es, but only the cells tagged with sufficient Epo survive the rapidly proliferating CFU-E phase to complete maturation. This reflects the experimental finding suggesting that Epo mediates apoptosis and, by interrupting the programmed cell death, controls the number of cells that mature (Adamson, 1995; Park, 1996).

Once precursor cells pass the CFU-E stage, they mature primarily by increasing their capacity to carry hemoglobin. These cells appear to proliferate without apoptosis, then stop dividing when they become reticulocytes—the final stage in the bone marrow. Epo appears to be able to accelerate the rate of proliferation and maturing during this stage of development. Reticulocytes accumulate hemoglobin and decrease their cell size, eventually losing their nuclei and their ability to produce proteins. When sufficiently small, the reticulocytes enter the bloodstream and become erythrocytes with a primary function of carrying O_2 to the tissues.

The schematic in Fig. 1 shows the primary features of our model with a few simplifications from the model presented below. Let $p(t, \mu)$ denote the population of precursor cells at time t with age μ, and let $V(E)$ be the velocity of maturation, which may depend on the hormone concentration, E. The maturity level, μ, for erythropoiesis can represent the accumulation of hemoglobin in the precursor cells. If $S_0(E)$ is the number of cells recruited into the proliferating precursor population, then the entry of new precursor cells into the age-structured model should satisfy the boundary condition:

$$V(E)p(t, 0) = S_0(E). \tag{1}$$

It is possible that cell proliferation is controlled by apoptosis, in which case $S_0(E)$ is simply a constant. Assume the birth rate for proliferating precursor cells is $\beta(\mu, E)$ and that $\alpha(\mu, E)$ represents the death rate from apoptosis. Let $h(\mu - \bar{\mu})$ be the distribution of maturity levels of the cells when released into the circulating blood, where $\bar{\mu}$ represents the mean age of mature precursor cells and

$$\int_0^{\mu_F} h(\mu - \bar{\mu})\, \mathrm{d}\mu = 1.$$

The disappearance rate function is given by:

$$H(\mu) = \frac{h(\mu - \bar{\mu})}{\int_{\mu}^{\mu_F} h(s - \bar{\mu})\, \mathrm{d}s}.$$

With these conditions the age-structured model for the population of precursor cells with $t > 0$ and $0 < \mu < \mu_F$ satisfies:

$$\frac{\partial p}{\partial t} + V(E)\frac{\partial p}{\partial \mu} = V(E)[\beta(\mu, E)p - \alpha(\mu, E)p - H(\mu)p]. \tag{2}$$

Let $m(t, v)$ be the population of mature non-proliferating cells at time t and age v. Assume that the mature cells age at a rate W, which is considered to be a constant for erythropoiesis since the aging process appears to depend only on the number of times that an erythrocyte passes through the capillaries. From the disappearance rate function, the boundary

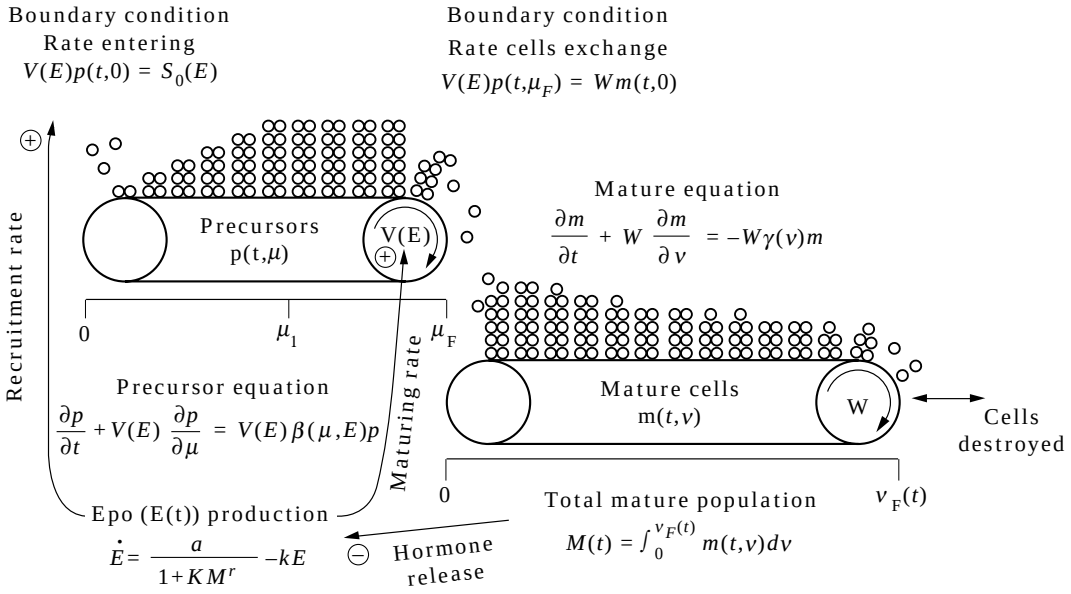

FIG. 1. Schematic representation of the age-structured model of erythropoiesis. For simplifying purposes, the model diagrammed includes neither the term for the apoptosis nor the distribution of maturation presented in the text, so agrees more closely to the model analysed and simulated later in the paper.

condition for cells entering the mature population is given by the following expression:

$$Wm(t, 0) = V(E) \int_0^{\mu_F} h(\mu - \bar{\mu}) p(t, \mu)\, \mathrm{d}\mu, \qquad (3)$$

where the maturity level μ_F represents the maximum age for a cell reaching maturity.

In the current formulation of the model, we consider that destruction of erythrocytes occurs by active removal of the oldest cells. By assuming either a constant supply of markers or a constant number of phagocytes that become satiated in their destruction of the oldest erythrocytes, there is a constant flux of erythrocytes from the mature population. This results in a moving boundary condition with the age of the oldest erythrocyte, $v_F(t)$, varying in t. The boundary condition, derived in Appendix A, is given by:

$$(W - \dot{v}_F(t)) m(t, v_F(t)) = Q, \qquad (4)$$

where Q is the fixed erythrocyte removal rate.

If $\gamma(v)$ is the death rate of mature cells (depending only on age), then the partial differential equation describing $m(t, v)$ is given by:

$$\frac{\partial m}{\partial t} + W \frac{\partial m}{\partial v} = -W\gamma(v)m, \quad t > 0, \quad 0 < v < v_F(t), \qquad (5)$$

where the maximum age, $v_F(t)$, is determined by (4).

The Epo level E is governed by a differential equation with a negative feedback, depending on the total population of mature cells, $M(t)$, defined by:

$$M(t) = \int_0^{v_F(t)} m(t, v)\, \mathrm{d}v. \qquad (6)$$

The differential equation for E is thus:

$$\frac{\mathrm{d}E}{\mathrm{d}t} = f(M) - kE, \qquad (7)$$

where k is the decay constant for the hormone and $f(M)$ is a monotone decreasing function of M representing the negative feedback effect of the total population of mature cells on the rate of hormone production. Typically, we shall consider the following form of f:

$$f(M) = \frac{a}{1 + KM^r}, \qquad (8)$$

which is a Hill function that often occurs in enzyme kinetic problems.

The partial differential equations and their boundary conditions given by eqns (1–5) describe the age-structured populations of the erythrocytes. The hormone erythropoietin is produced at a rate dependent on the total mature erythrocyte population given by (6), and exerts control in the age-structured model through the boundary conditions, the birth and death of precursor cells, and the velocity of aging. This system of equations may be transformed to a system of threshold delay equations following the techniques of several authors (Bélair *et al*., 1995; Gatica & Waltman, 1982, 1988; Metz & Diekmann, 1986; Smith, 1993). This technique assumes that a solution to (7) for $E(t)$ is known, then the method of characteristics for the partial differential equations (2) and (5) is used to find solutions $p(t, \mu)$ and $m(t, v)$. See Appendix B for the general solution. When only long time behavior is considered, the partial differential equations reduce to a system of integro-differential equations or threshold-type delay equations with the state-dependent delay τ defined implicitly by

$$\mu = \int_{t-\tau}^{t} V(E(r))\, \mathrm{d}r. \qquad (9)$$

3. Reduction to a Delay Differential System with State Dependent Delay

In the previous section and Appendix B, the age-structured model was reduced to a system of threshold-type delay equations. In this section, a few simplifying assumptions that are reasonable for erythropoiesis are made that further reduce this system to a system of delay differential equations with a fixed delay in one equation and a state dependent delay in an equation governing the age at which mature erythrocytes die. These assumptions parallel the ones that Bélair *et al*. (1995) used to show how the age-structured model can be reduced to a system of delay differential equations with two delays. See that work for more details justifying the assumptions.

The first assumption is that the velocities of aging are constant and normalized to one, i.e.

$$V(E) = 1 \quad \text{and} \quad W = 1.$$

This assumption significantly simplifies the expressions for $p(t, \mu)$ and $m(t, v)$ found in Appendix B [eqns (B.1) and (B.2)]. Furthermore, it reduces (9) to $\tau = \mu$. The second assumption is that the precursor cells grow exponentially for a given period of time μ_1,

then stop dividing. This assumption on the birth rate of the precursor cells yields

$$\beta(\mu, E) = \begin{cases} \beta, & \mu < \mu_1, \\ 0, & \mu \geqslant \mu_1, \end{cases} \tag{10}$$

for some constant growth rate β. If we assume that apoptosis occurs at the beginning of the life cycle of the precursor population, then the disappearance function $\alpha(\mu, E)$ can be included in the boundary condition $S_0(E)$. Similarly, if $h(\mu - \bar{\mu})$ is a Dirac δ-function, then the changing of precursor cells into mature erythrocytes only occurs on the boundary.

With these assumptions it follows that the solution for $M(t)$, given by (B.3), can be written as

$$M(t) = \int_0^{v_F(t)} e^{\beta\mu_1} S_0(E(t - v - T)) e^{-\gamma v}\, \mathrm{d}v,$$

where $T = \mu_F$. Differentiating this equation yields

$$\frac{\mathrm{d}M(t)}{\mathrm{d}t} = e^{\beta\mu_1}[S_0(E(t - T)) - e^{-\gamma v_F(t)}(1 - \dot{v}_F(t)) S_0(E(t - T - v_F(t)))] - \gamma M(t). \tag{11}$$

The assumptions on W, h, and the evaluation of p transform the constant flux boundary condition to

$$Q = (1 - \dot{v}_F(t)) e^{\beta\mu_1} e^{-\gamma v_F(t)} S_0(E(t - T - v_F(t))). \tag{12}$$

By substituting (12) into (11), we obtain the following system of delay differential equations with a fixed delay T and a state dependent delay occurring in the equation governing the age at which mature cells die:

$$\begin{aligned} \frac{\mathrm{d}M(t)}{\mathrm{d}t} &= e^{\beta\mu_1} S_0(E(t - T)) - \gamma M(t) - Q, \\ \frac{\mathrm{d}E(t)}{\mathrm{d}t} &= f(M(t)) - kE(t), \\ \frac{\mathrm{d}v_F(t)}{\mathrm{d}t} &= 1 - \frac{Q e^{-\beta\mu_1} e^{\gamma v_F(t)}}{S_0(E(t - T - v_F(t))}. \end{aligned} \tag{13}$$

Two significant points can be made about (13). First, the equation for $\dot{M}(t)$ reduces to having only the single time delay T, exponential decay, and the constant flux $-Q$. The production term represents a delayed entrance after fixed exponential growth of the BFU-Es that were recruited to mature. The constant flux, $-Q$, matches our "satiated predator" assumption that a constant number of red blood cells are destroyed by the macrophages.

Second, we observe that the $\dot{v}_F(t)$ equation is uncoupled from the other two equations. Thus, despite its greater complications because of the state dependent delay, this equation has no effect on the behavior of the solutions of the remaining (two equation) system. This is due to the constant Q of the first equation "hiding" the variability of the longest maturation time, $v_F(t)$.

4. Linear Stability Analysis

In this section we examine the linear stability of the simplified model given by (13). Experimental results (Clarke & Housmann, 1977) show that $S_0(E)$ is monotonically increasing, and in fact, almost linear for a wide range of E. The function $f(M)$ represents the negative feedback by M in the production of E, so is monotonically decreasing. Thus, there is a unique equilibrium $(\bar{M}, \bar{E}, \bar{v}_F)$ for (13).

The simplified model given by (13) can be linearized about its equilibrium, and the resulting system is given by:

$$\begin{aligned} \dot{M}(t) &= e^{\beta\mu_1} S_0'(\bar{E}) E(t - T) - \gamma M(t), \\ \dot{E}(t) &= f'(\bar{M}) M(t) - kE(t), \\ \dot{v}_F(t) &= \frac{1}{\bar{E}} E(t - T - \bar{v}_F) - \gamma v_F(t). \end{aligned} \tag{14}$$

Notice that the linearization of the last equation can be justified (Cooke & Huang, 1996) despite additional difficulties due to the state-dependence of the delay v_F.

The characteristic equation for the eigenvalues corresponding to (14) is given by

$$\det \begin{vmatrix} \lambda + \gamma & -e^{\beta\mu_1} S_0'(\bar{E}) e^{-\lambda T} & 0 \\ -f'(\bar{M}) & \lambda + k & 0 \\ 0 & -\dfrac{1}{\bar{E}} e^{-\lambda(T + \bar{v}_F)} & \lambda + \gamma \end{vmatrix} = 0,$$

which can be written

$$(\lambda + \gamma)[(\lambda + \gamma)(\lambda + k) + Ae^{-\lambda T}] = 0,$$

where $A \equiv -e^{\beta\mu_1} S_0'(\bar{E}) f'(\bar{M}) > 0$. One solution of this equation is $\lambda = -\gamma$, associated with the v_F equation, which is shown to be inherently stable. It remains to analyse the exponential polynomial

$$(\lambda + \gamma)(\lambda + k) = -Ae^{-\lambda T}, \tag{15}$$

to determine for which parameter values all its roots have negative real parts.

Equation (15) has been studied extensively (see Boese & van den Driessche (1984), Cooke & Grossman (1982) and Mahaffy (1982) and references therein). In most of these studies, when a systematic investigation of the parameter values yielding stability of the equilibrium is performed, one of the bifurcation parameters is the time delay T. Our analysis differs slightly, since here the delay T is known. Thus, we use

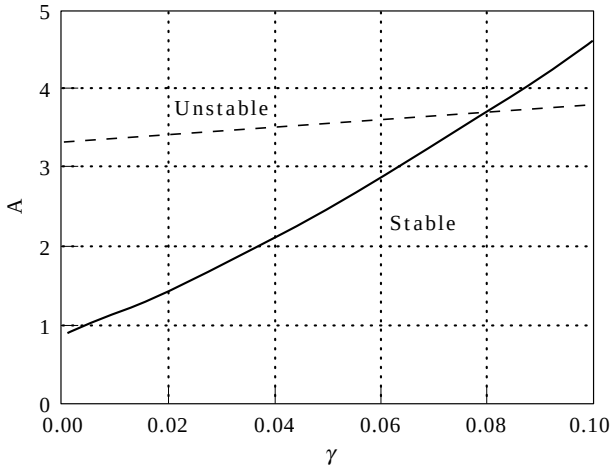

FIG. 2. Stability region for the basic model in the place of the parameters A and γ. A super-critical Hopf bifurcation occurs along the dotted line, and the equilibrium $(\bar{M}, \bar{E}, \bar{v}_F)$ is stable for positive values of A below this line. The full line displays the location of the equilibrium for the rabbit experiment as γ varies.

the parameters A and γ as bifurcation parameters. We also assume that the remaining parameters are constant, at values to be discussed in the following section. Only their signs are assumed for the moment with both k and T positive.

A root of eqn (15) only acquires a positive real part by crossing the imaginary axis. A zero root $\lambda = 0$ occurs when $A = -k\gamma$, which is impossible in the first quadrant of the parameter plane (γ, A), since both A and γ are non-negative. For purely imaginary roots $\lambda = i\omega$, substituting $\lambda = i\omega$ into eqn (15) and separating real and imaginary parts yields

$$\begin{aligned} A\cos\omega T + k\gamma - \omega^2 &= 0, \\ -A\sin\omega T + \omega\gamma + k\omega &= 0. \end{aligned} \tag{16}$$

These two equations can be considered as a linear system of equations in the two unknowns A and γ and inverted to

$$\begin{aligned} A &= (\omega^2 + k^2)/D, \\ \gamma &= (\omega\sin\omega T - k\cos\omega T)/D, \end{aligned} \tag{17}$$

where $D = 1/(\cos\omega T + k\sin\omega T/\omega)$.

Thus, in the plane of the parameters (γ, A) we obtain the entire locus of purely imaginary roots of eqn (15). The stability region is illustrated in Fig. 2, using parameter values for the simulation of a rabbit with induced auto-immune hemolytic anemia described at the beginning of Section 5.2. Notice that for all values of γ, a sufficiently small value of A leads to a stable equilibrium. At any fixed value of A, an increase in the value of γ eventually leads to a stabilization of the equilibrium. It is possible to show that stability of the equilibrium is lost via a supercritical Hopf bifurcation (Bélair, 1996). A locally stable limit cycle appears for parameter values above the line where purely imaginary roots exist. A comparison of the bifurcation diagram in Fig. 2 with the one presented in fig. 6 of Bélair *et al*. (1995) gives a remarkably similar value for the bifurcation point for the rabbit experiment near $\gamma = 0.08$.

5. Simulations of the Mathematical Model

In this section, the mathematical model given by (13) is simulated for two cases and compared with previous results of Bélair *et al*. (1995), where the mature cells had a fixed lifespan. Our first example examines the response of a normal human subject following a blood donation of 5% of the blood (a mild form of phlebotomy). The second example is based on experiments of Orr *et al*. (1968), who studied rabbits with an induced auto-immune hemolytic anemia that exhibit periodic oscillations in their erythrocyte populations.

5.1. HUMAN BLOOD DONATION

A normal human has approximately 3.5×10^{11} erythrocytes kg^{-1} body weight and a mean Epo concentration of around 10 mU ml^{-1} of plasma. Our model assumes $\bar{M} = 3.5$ and $\bar{E} = 10$. The maturation of red blood cell precursors takes about 6 days and mature erythrocytes live on average 120 days, so we assume $T = 6$ and $\bar{v}_F = 120$. Since the half-life of Epo is about 6 hr and only 0.06–0.4% of mature cells are destroyed by normal physiological activity, we assume that $k = 2.8$ and $\gamma = 0.001$. Using a least squares fit to data of Erslev (1991), we found the parameters in the Hill function (8) to satisfy $a = 6570$, $K = 0.0382$, and $r = 6.96$. From the steady-state values it follows that $S_0'(\bar{E}) = 0.0031$ and $Q = 0.0275$.

With these parameters and the assumption that $S_0(E)$ is a linear function, we simulated this model for 300 days following a blood donation. The numerical method employed in this simulation was a modified fourth order Runge–Kutta scheme with fixed stepsize. In the simulation, the history of $E(t)$ is sorted on a fixed grid, and a linear interpolation is used to determine intermediate values between grid points as the delay, $T + v_F(t)$, varies in the state dependent delay equation of system (13).

A typical blood donation causes approximately 5% of the erythrocytes to be lost. To account for this in the simulation of (13), the initial data is taken as $M(0) = 0.95\bar{M}$. In addition, the history of $E(t)$ must be adjusted to account for the loss of mature cells originally stimulated by $S_0(E)$. Thus, $E(t) = 0.95\bar{E}$ for

$-\bar{v}_F \leqslant t < -T$, while $E(t) = \bar{E}$ for $-T \leqslant t \leqslant 0$ as the precursor population residing in the bone marrow is initially unaffected by a blood donation which harvests only circulating erythrocytes.

The simulation of (13) is shown in Fig. 3 with the previous results of Bélair *et al*. (1995) overlaid for comparison. The only difference between (13) and the earlier model is the boundary condition affecting the death of aged erythrocytes. The previous model assumed that all erythrocytes die at 120 days, which causes a renewed decline in erythrocytes near 126 days. In the new model (13), with the constant flux boundary condition resulting from mature erythrocytes being actively destroyed, the erythrocyte population levels off at the equilibrium value. It can be seen that 99% of the equilibrium value is restored within 18 days. This is consistent with the accepted value (Guyton & Hall, 1996) of 3 to 6 weeks for total recovery of red blood cell concentration following a blood donation. The simulations of Fig. 3 comparing the earlier predictions of Bélair *et al*. (1995) with the predictions of the refined model presented here suggest that the current formulation is physiologically more realistic.

The actual variation in $v_F(t)$ is very small over the course of the simulation with a total variation of only 6 days as shown in Fig. 4. $v_F(t)$ begins by slowly dropping from 120 to a minimum of 114.34 in 115 days. This decline is due to the loss from all age classes from the blood donation. Then $v_F(t)$ rises more rapidly to a maximum of 120.02 at 157 days, which is several days after the new erythrocytes produced after the blood donation have aged to the point of death. The reported range for the age at death for

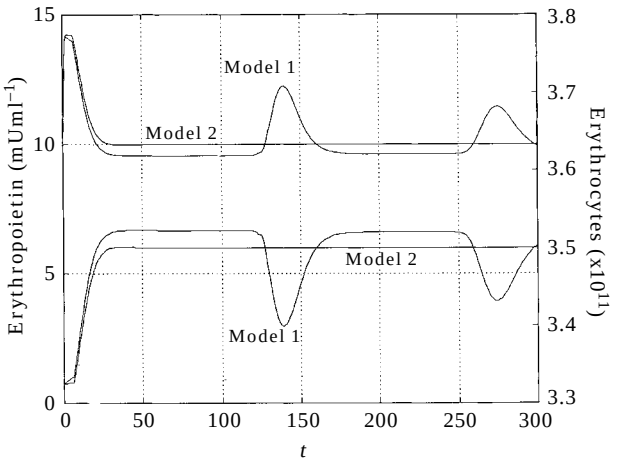

FIG. 3. Simulation of the model showing the concentration of Epo and the population of mature erythrocytes following a 5% blood donation at $t = 0$. The graphs labeled Model 1 are simulations from previous work where the mature cells die at 120 days, while the graphs labeled Model 2 are from (13).

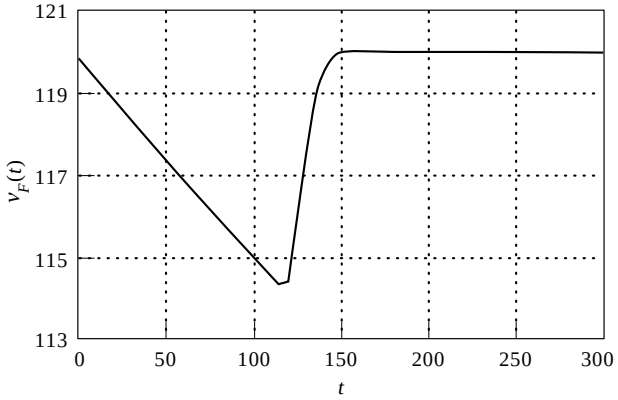

FIG. 4. This graph shows the variation of the age of the mature erythrocytes ($v_F(t)$) for the simulation shown in Fig. 3.

mature erythrocytes is from 100 to 140 days (Erslev & Beutler, 1995), so the variation in our model is far less than experimentally observed values. It is interesting that a slow change in the delay can produce such a dramatic difference in the behavior of the dynamical system.

5.2. INDUCED AUTO-IMMUNE HEMOLYTIC ANEMIA

In the experiments of Orr *et al*. (1968), rabbits were continuously given red blood cell iso-antibody for prolonged periods of time. As a consequence, there were oscillations in their circulating reticulocyte counts and in their hemoglobin levels with an approximate period of 18 days. (The dashed line in Fig. 6 is a reconstruction of their hemoglobin data of Fig. 3 plotted as a percentage of normal values.) These data strongly suggest the presence of periodic oscillations in erythrocyte populations for rabbits regularly given an iso-antibody to their red blood cells. This experimentally induced auto-immune response is assumed to cause a random destruction of erythrocytes, which is reflected in our model by an increase in γ. Figure 2 shows that a Hopf bifurcation occurs near $\gamma = 0.08$ for the model of these rabbits with an auto-immune induced hemolytic anemia given the parameters listed below.

For comparative purposes, the parameters in (13) for the simulation of the rabbit experiment were initially chosen to agree with Bélair *et al*. (1995). The experimental work of Orr *et al*. (1968) indicated the average erythrocyte population was 75% of normal, so we chose $\bar{M} = 2.63(\times 10^{11}$ erythrocytes kg^{-1} body wt) and $\bar{E} = 71.1$ (mU ml^{-1} plasma). Orr *et al*. (1968) claim the maturation for rabbit erythrocytes, T, is 3 days, which was the value used in Bélair *et al*. (1995) and so is used for our comparative study below. However, other references suggest that this value is too low, so additional simulations are performed and

analysed with other values of T. The normal rabbit erythrocyte lifespan is $\bar{v}_F = 50$ days (Burwell *et al.*, 1953). Using data for rats (Orr *et al.*, 1968), we chose $k = 6.65\,\text{day}^{-1}$. The Hill function parameters used were $r = 6.96$, $K = 0.0382$, and $a = 15{,}600$. The parameter γ is increased from its normal value in the previous simulation to reflect the higher destruction rate. This parameter has a significant effect on the amplitude of the simulation and is found to correspond well to the experiments of Orr *et al.* (1968) when $\gamma = 0.1$. From the steady state information it follows that $S_0'(\bar{E}) = 0.00372$ and $Q = 0.00178$.

For our numerical simulation we begin with initial data at normal levels, *i.e.*, $M(0) = 3.5$, $v_f(0) = 50$, and $E(t) = 10$ for $t \in [-T - v_F(0), 0]$. With the parameters given in the previous paragraph, a Runge–Kutta integration scheme is applied to the models, and the simulations are shown in Fig. 5. The simulations of Bélair *et al.* (1995) and the one for (13) are readily seen to be very close. After 90 days of simulation the solution has shifted by approximately 1 day, but the amplitude of oscillation is virtually the same. Initially, the length of the age for the mature cells varies quite dramatically with $v_F(t)$ dropping as low as 30.7 by the 34th day. However, after 80 days the model settles into very regular oscillations in all variables, and $v_F(t)$ oscillates between 48.5 and 52.8 with the same period as the other variables. Again the state dependent delay $v_F(t)$ responds very conservatively in this model when compared to the variation in the mature population, $M(t)$, and the concentration of Epo, $E(t)$. The oscillations in our model have a period of 11–12 days, compared to 16–17 days in the experiments, and an amplitude that is slightly lower and more regular than the experimental results.

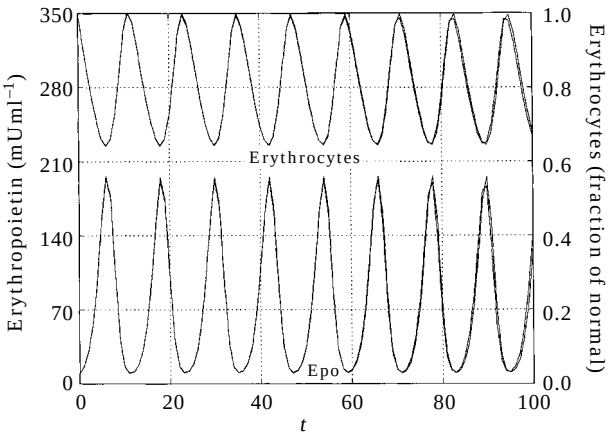

FIG. 5. Comparative simulations of models for a rabbit with an auto-immune induced hemolytic anemia showing the concentration of Epo and the fraction of mature erythrocytes relative to normal erythrocyte population. The model of eqn (13) is compared with the two-delay model in Bélair *et al.* (1995).

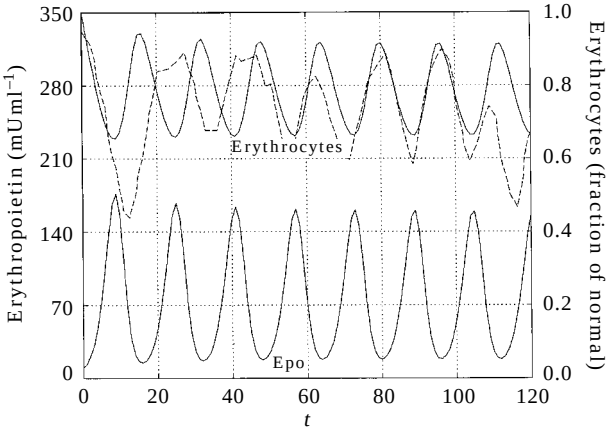

FIG. 6. Comparative study of the model predictions of eqn (13) to the hemoglobin data (dashed line) of Orr *et al.* (1968) for a rabbit with an auto-immune induced hemolytic anemia with maturation delay $T = 4.1$ and $\gamma = 0.065$. The simulation shows the concentration of Epo and the fraction of mature erythrocytes relative to normal populations.

As noted earlier, the maturation time for rabbit erythrocytes may be higher than the value used for the simulations in Fig. 5. Further simulations varying the maturation time, T, show that the period of oscillation in the model is very sensitive to this parameter. For example, if we choose the human maturation time, $T = 6$, then the period of oscillation changes to 23.5 days for (13). To obtain a similar amplitude of oscillation, γ changes to about 0.045 along with corresponding changes to $S_0'(\bar{E})$ and Q. If these parameter values are used in the model of Bélair *et al.* (1995), then the period is 22 days and the amplitude is reduced to 84% of the amplitude for the simulation of (13). Since the bifurcation diagram (Fig. 6) in Bélair *et al.* (1995) is more complicated than Fig. 2, we would predict that the models would diverge as γ decreases. The numerical simulations indicate that the two delay model is slightly more stable than (13) though the behavior remains similar. Our simulation with $T = 6$ begins with $v_F(t)$ decreasing to a minimum of 15.1 days before returning to an oscillatory solution with $v_F(t)$ between 46.8 and 54.1. The initial decline appears to be unrealistic.

If we keep all parameters at their previous values but adjust T and γ to yield simulations close to the experiments, then we found (see Fig. 6) that $T = 4.1$ days and $\gamma = 0.065$ yield results with a period of 16.5 days and an amplitude that is quite comparable to the experiment of Orr *et al.* (1968), if one ignores what appears to be a transient effect in the first 40–50 days of their data. This suggests that our model provides a partial, but indirect, means of estimating the time of maturation and rate of destruction of erythrocytes.

Because the experiment induces an anemia, which results in an increase in Epo, it is possible that this experiment has an accelerated maturation time (smaller delay T than normal) as discussed in Section 2. However, many other parameters are in this model, and our studies have not been exhaustive.

6. Discussion

The age-structured hematopoiesis model developed in this paper, and specifically applied to erythropoiesis, contains a novel boundary condition which corresponds to a constant flux of erythrocytes as mature cells are actively destroyed by macrophages. (In an ecological framework, this condition is equivalent to having a constant number of predators that are constantly satiated and control the population by consuming the oldest individuals in the population). This modification transforms the model of Bélair *et al*. (1995) with two delays into a system of three delay differential equations with a state-dependent delay. However, this greater complexity is readily simplified, and a much simpler system of two equations with only one delay has been analysed for stability. Our analysis shows exactly what assumptions are necessary to reduce the age-structured population model to a system of delay differential equations that are significantly easier to analyse as shown by the Hopf bifurcation analysis of Section 4.

The numerical simulations of the model presented in Section 5.1 demonstrate the behavior expected following the daily procedure of a blood donation, where initially the population drops significantly. The Epo concentration is predicted to rapidly rise, which causes the erythrocyte population to recover and tend toward equilibrium. The delay variable, describing how long the mature erythrocytes live, recovers slowly as it controls the history of the age-structured population. All of these variables are, in theory, clinically measurable. It would be rather exciting if data on Epo levels and erythrocyte number were collected at a sufficiently high sampling frequency to allow a quantitative comparison between the data and the predictions of the model. Only in this way can modelers hope to refine models such as these to accurately reflect the experimental/clinical reality. In a similar vein, the predictions of the simulations of Section 5.2 are well within the realm of checking from an experimental point of view, and logistically would be easier to carry out on a laboratory animal than on a human. One can only hope that experimental hematologists will be sufficiently intrigued by modelers' predictions to join forces and work toward a better understanding of the hematopoietic regulatory system. Mathematically, the extension of this paper offers a significant improvement in the predicted response to blood donation (see Section 5.1), but has a negligible effect on the simulations related to the laboratory induced autoimmune hemolytic anemia (see Section 5.2). One facet of erythropoiesis (and hematopoiesis in general) that has not been considered here involves the effects of "random" fluctuations in the system or other dynamic control systems and how these would be manifested in the model behavior. Little is known about the degree of variation in the number of circulating blood cells in single mammals over time, though preliminary data taken on one of the authors (JMM) indicates that under certain circumstances it may be considerable. This question of the normal degree of variation in blood cell numbers is unexplored in the clinical/laboratory literature, and from a modeling perspective the understanding of the effects of additive and/or multiplicative noise on the behavior of functional equations or differential delay equations is in its infancy (Mackey & Nechayeva, 1994, 1995).

The model presented in this paper is sufficiently general that it can, we feel, easily be applied to other hematopoietic regulatory situations, e.g., the regulation of platelet production via thrombopoietin, and the regulation of white blood cell production by the colony stimulating factors and other cytokines (Mackey, 1996). The constant flux boundary condition introduced here probably captures the physiological reality of peripheral, circulating blood cell destruction better than have previous models (Dunn, 1983; Kirk *et al*., 1968; Mackey, 1978, 1979a,b, 1996; Mackey & Milton, 1990; Morley, 1979; Wichmann & Loeffler, 1988), and it will be of particular interest to see whether this improvement will significantly aid in the explanation of one of the most mysterious of the periodic hematological disorders: the cyclical thrombocytopenias (Bernard & Caen, 1962; Brey *et al*., 1969; Caen *et al*., 1964; Cohen & Cooney, 1974; Demmer, 1920; Engstrom *et al*., 1966; Goldsmith & Fono, 1972; Lewis, 1974; Skoog *et al*., 1957; Wasatjerna, 1967; Wilkinson & Firkin, 1966) which have, to date, resisted all modeling attempts.

This work was supported in part by NSF (JMM), NSERC (JB and MCM) and FCAR (JB and MCM). Part of this work was performed when JMM was visiting the Centre de Recherches Mathématiques and the Montréal based Centre for Nonlinear Dynamics Physiology and Medicine.

REFERENCES

Adamson, J. W. (1995). The relationship of erythropoietin and iron metabolism to red blood cell production in humans. *Sem. Oncol.* **21,** 9–15.

Bélair, J. (1997). Stability analysis of an age-structured model with a state-dependent delay. *Can. Applied Math* (in press).

Bélair, J., Mackey, M. & Mahaffy, J. M. (1995). Age-structured and two-delay models for erythropoiesis. *Math. Biosci.* **128,** 317–346.

Bernard, J. & Caen, J. (1962). Purpura thrombopénique et megacaryocytopénie cycliques mensuels. *Nouv. Rev. franc. Hémat.* **2,** 378–386.

Boese, F. & van den Driessche, P. (1994). Stability with respect to the delay in a class of differential-delay equations. *Can. Applied Math. Quart.* **2,** 151–175.

Brey, O., Garner, E. P. R. & Wells, D. (1969). Cyclic thrombocytopenia associated with multiple antibodies. *Brit. Med. J.* **3,** 397–398.

Burwell, E. L., Brickley, B. A. & Finch, C. A. (1953). Erythrocyte life span in small mammals. *Amer. J. Physiol.* **172,** 718.

Caen, J., Meshaka, G., Larrieu, M. J. & Bernard, J. (1964). Les purpuras thrombopéniques intermittents idiopathiques. *Sem. Hop. Paris.* **40,** 276–282.

Chikkappa, G., Borner, G., Burlington, H., Chanana, A. D., Cronkite, E. P., Ohl, S., Pavelec, M. & Robertson, J. S. (1976). Periodic oscillation of blood leukocytes, platelets, and reticulocytes in a patient with chronic myelocytic leukemia. *Blood* **47,** 1023–1030.

Clarke, B. J. & Housmann, D. (1977). Characterisation of an erythroid precursor cell of high proliferative capacity in normal human peripheral blood. *Proc. Natl. Acad. Sci. U.S.A.* **74,** 1105–1109.

Cohen, T. & Cooney, D. P. (1974). Cyclical thrombocytopenia: Case report and review of literature. *Scand. J. Haemat.* **12,** 9–17.

Cooke, K. & Grossman, Z. (1982). Discrete delay, distributed delay and stability switches. *J. Math. Anal. Appl.* **86,** 592–627.

Cooke, K. & Huang, W. (1996). On the problem of linearization for state-dependent delay differential equations. *Proc. AMS* **124,** 1417–1426.

Crichton, M. (1995). *The Lost World*. Viking Press, New York.

Dale, D. C. & Hammond, W. P. (1988). Cyclic neutropenia: A clinical review. *Blood Reviews* **2,** 178–185.

Delobel, J., Charbord, P., Passa, P. & Bernard, J. (1973). Evolution cyclique spontanée de la leucocytose dans un cas de leucémie myéloide chronique. *Nouv. Rev. franc Hémat.* **13,** 221–228.

Demmer, T. (1920). Morbus maculosus werlhofii in regelmassigen vierwochentlichen schuben bei einem 60 jahrigen mann, nebst untersuchungen uber die blutplattchen. *Folia Haemat.* **26,** 74–86.

Dunn, C. D. R. (1983). Cyclic hematopoiesis: The biomathematics. *Exp. Hematol.* **11,** 779–791.

Engstrom, K., Lundquist, A. & Soderstrom, N. (1966). Periodic thrombocytopenia or tidal platelet dysgenesis in a man. *Scand. J. Haemat.* **3,** 290–292.

Erslev, A. J. (1991). Erythropoietin titers in health and disease. *Sem. Hematol.* **28** Suppl. 3, 2–8.

Erslev, A. J. & Beutler, E. (1995). Production and destruction of erythrocytes. In: *William's Hematology* (Beutler, E., Lichtman, M. A., Coller, B. S. & Kipps, T. J., eds) Chapter 39. New York, McGraw-Hill Inc.: 5th Edn

Evan, G. I., Brown, L., Wyte, M. & Harrington, E. (1995). Apoptosis and the cell cycle. *Curr. Opinion in Biol.* **7,** 825–834.

Gatica, J. A. & Waltman, P. (1982). A threshold model of antigen antibody dynamics with fading memory. In: *Nonlinear Phenomena in Mathematical Sciences* (Lakshmikantham, V., ed.). New York, Academic Press.

Gatica, J. A. & Waltman, P. (1988). A system of functional differential equations modeling threshold phenomena. *Appl. Anal.* **28,** 39–50.

Gatti, R. A., Robinson, W. A., Deinare, A. S., Nesbit, M., McCullough, J. J., Ballow, M. & Good, R. A. (1973). Cyclic leukocytosis in chronic myelogenous leukemia. *Blood* **41,** 771–782.

Goldschmidt, B. & Fono, R. (1972). Cyclic fluctuations in platelet count, megakaryocyte maturation and thrombopoietin activity in cyanotic congenital heart disease. *Acta Paediat. Scand.* **61,** 310–314.

Gordon, R. R. & Varadi, S. (1962). Congenital hypoplastic anemia (pure red cell anemia) with periodic erythroblastopenia. *Lancet* **i,** 296–299.

Guyton, A. C. & Hall, J. E. (1996). *Textbook of Medical Physiology*. Philadelphia: W. B. Saunders.

Jones, J. B. & Lange, R. D. (1983). Cyclic hematopoiesis: Animal models. *Imunol. Hematol. Res. Monographs* **1,** 33–42.

Kazarinoff, N. D. & van den Driessche, P. (1979). Control of oscillations in hematopoiesis. *Science* **203,** 1348–1350.

Kennedy, B. J. (1970). Cyclic leukocyte oscillations in chronic myelogenous leukemia. *Blood* **35,** 751–760.

King-Smith, E. A. & Morley, A. (1970). Computer simulation of granulopoiesis: Normal and impaired granulopoiesis. *Blood* **36,** 254–262.

Kirk, J., Orr, J. S. & Hope, C. S. (1968). A mathematical analysis of red blood cell and bone marrow stem cell control mechanisms. *Br. J. Haematol.* **15,** 35–46.

Koury, M. J. (1992). Programmed cell death (apoptosis) in hematopoiesis. *Exp. Hematol.* **20,** 391–394.

Lange, R. D. (1983). Cyclic hematopoiesis: Human cyclic neutropenia. *Exp. Hematol.* **11,** 435–451.

Lewis, M. L. (1974). Cyclic thrombocytopenia: A thrombopoietin deficiency? *J. Clin. Path.* **27,** 242–246.

Mackey, M. C. (1978). A unified hypothesis for the origin of aplastic anemia and periodic haematopoiesis. *Blood* **51,** 941–956.

Mackey, M. C. (1979a). Dynamic haematological disorders of stem cell origin. In: *Biophysical and Biochemical Information Transfer in Recognition* (Vassileva-Popova, J. G. & Jensen, E. V., eds), pp. 373–409. New York: Plenum Publishing Corp.

Mackey, M. C. (1979b). Periodic auto-immune hemolytic anemia: An induced dynamical disease. *Bull. Math. Biol.* **41,** 829–834.

Mackey, M. C. (1997). Mathematical models of hematopoietic cell replication control. In: *The Art of Mathematical Modeling*: *Case Studies in Ecology*, *Physiology and Biofluids* (Othmer, H. G., Adler, F. R., Lewis, M. A. & Dallon, J. C., eds). Prentice Hall, in press.)

Mackey, M. C. & Milton, J. G. (1990). Feedback, delays, and the origin of blood cell dynamics. *Comm. on Theor. Biol.* **1,** 299–327.

Mackey, M. C. & Nechayeva, I. G. (1994). Noise and stability in differential delay equations. *J. Dynam. and Diff. Eqns.* **6,** 395–426.

Mackey, M. C. & Nechayeva, I. G. (1995). Solution moment stability in stochastic differential delay equations. *Phys. Rev. E.* **52,** 3366–3376.

Mahaffy, J. M. (1982). A test for stability of linear differential delay equations. *Quart. Appl. Math.* **40,** 193–202.

Mastrangelo, R., Stabile, A., Parenti, D. & Segni, G. (1974). Spontaneous leukocyte oscillation during blastic crisis of chronic myeloid leukemia. *Cancer* **33,** 1610–1614.

Mastrangelo, R., Stabile, A., Parenti, D. & Cimatti, G. (1976). A specific spontaneous leukocyte cycle in chronic myelogenous leukemia. *Tumori* **62,** 197–204.

Metz, J. A. J. & Diekmann, O. (1986). *The Dynamics of Physiologically Structured Populations*, Vol. 68. Lecture Notes in Biomathematics. Berlin: Springer-Verlag.

Milton, J. G. & Mackey, M. C. (1989). Periodic haematological diseases: Mystical entities or dynamical disorders? *J. Roy. Coll. Phys.* (*Lond.*) **23,** 236–241.

Morley, A. (1970). Periodic diseases, physiological rhythms and feedback control—a hypothesis. *Aust. Ann. Math.* **3,** 244–249.

Morley, A. (1979). Cyclic hemopoiesis and feedback control. *Blood Cells* **5,** 283–296.

Morley, A. A., Baikie, A. G. & Galton, D. A. G. (1967). Cyclic leukocytosis as evidence for retention of normal homeostatic control in chronic granulocytic leukaemia. *Lancet*, 1320–1322.
Nowell, P. C., Jackson, L., Weiss, A. & Kurzrock, R. (1988). Historical communication: Philadelphia-positive chronic myelogenous leukemia followed for 27 years. *Cancer Genetics & Cytogenetics* **34,** 57–61.
Orr, J. S., Kirk, J., Gray, K. G. & Anderson, J. R. (1968). A study of the interdependence of red cell and bone marrow stem cell populations. *Br. J. Haemat*. **15,** 23–34.
Park, J. R. (1996). Cytokine regulation of apoptosis in hematopoietic precursor cells. *Curr. Opinion in Hematol*. **3,** 191–196.
Ranlov, P. & Videbaek, A. (1963). Cyclic haemolytic anaemia synchronous with Pel-Ebstein fever in a case of Hodgkin's disease. *Acta Med. Scand*. **174,** 583–588.
Rodriguez, A. R. & Lutcher, C. L. (1976). Marked cyclic leukocytosis leukopenia in chronic myelogenous leukemia. *Am. J. Med*. **60,** 1041–1047.
von Schulthess, G. K. & Mazer, N. A. (1982). Cyclic neutropenia (CN): A clue to the control of granulopoiesis. *Blood* **59,** 27–37.
Shadduck, R. K., Winkelstein, A. & Nunna, N. G. (1972). Cyclic leukemia cell production in CML. *Cancer* **29,** 399–401.
Skoog, W. A., Lawrence, J. S. & Adams, W. S. (1957). A metabolic study of a patient with idiopathic cyclical thrombocytopenic purpura. *Blood* **12,** 844–856.
Smith, H. L. (1993). Reduction of structured population models to threshold-type delay equations and functional differential equations: A case study. *Math. Biosci*. **113,** 1–23.
Steinbach, K. H., Raffler, H., Pabst, G. & Fliedner, T. M. (1980). A mathematical model of canine granulocytopoiesis. *J. Math. Biol*. **10,** 1–12.
Symmans, W. A., Beresford, C. H., Bruton, D., Despommier, D. D., Dickson, D., Linehan, B. J., Reeder, W. J. & Shepherd, C. S. (1986). Cyclic eosinophilic myositis and hyperimmunoglobulin-E. *Ann. Int. Med*. **104,** 26–32.
Umemura, T., Hirata, J., Kaneko, S., Nishimura, J., Motomura, S., Kozuru, M. & Ibayashi, H. (1986). Periodical appearance of erythropoietin-independent erythropoiesis in chronic myelogenous leukemia with cyclic oscillation. *Acta Haematologica* **76,** 230–234.
Wasastjerna, C. (1967). Cyclic thrombocytopenia of acute type. *Scand. J. Haemat*. **4,** 380–384.
Wazewska-Czyzewska, M. (1984). *Erythrokinetics*, Warsaw, PKiN.
Wheldon, T. E., Kirk, J. & Finlay, H. M. (1974). Cyclical granulopoiesis in chronic granulocytic leukemia: A simulation study. *Blood* **43,** 379–387.
Wheldon, T. E. (1975). Mathematical models of oscillatory blood cell production. *Math. Biosci*. **24,** 289–305.
Wichmann, H. E. & Loeffler, M. (1988). *Mathematical Modeling of Cell Proliferation*: *Stem Cell Regulation in Hemopoiesis*. Boca Raton: CRC Press.
Wilkinson. T. & Firkin, B. (1966). Ideopathic cyclical acute thrombocytopenic purpura. *Med. J. Aust*. **1,** 217–219.
Wright, D. G., Dale, D. C., Fauci, A. S. & Wolff, S. M. (1981). Human cyclic neutropenia: clinical review and long term follow up of patients. *Medicine* **60,** 1–13.
Yamauchi, K. & Ide, A. (1992). Spontaneous remission with cyclic leukocytosis in chronic myelogenous leukemia. *Acta Haematological* **88,** 136–138.
Yuan, J. (1995). Molecular control of life and death. *Curr. Opinion in Cell Biol*. **7,** 211–214.

APPENDIX A

Constant Flux Boundary Condition

The boundary condition given by eqn (4) is needed in this model to account for the loss of mature erythrocytes. When erythrocytes age, their cell membrane breaks down and macrophages destroy the least pliable cells. We assume that the macrophages are in constant supply and are saturated in their consumption of erythrocytes, which allows the age of destruction of erythrocytes to vary. This condition is the one obtained in predator-prey models where the prey far outnumber the predators, so predators could always eat their fill. There is then a saturation, or satiation effect in the predators, their intake is constant and targeted at the weakest, oldest prey.

Figure A1 shows a schematic representation of the boundary condition. The conveyor belt advances at speed W, and the belt is allowed to either stretch or shrink such that the flux lost from the mature population remains constant. Let Q be the rate of removal of erythrocytes: then $Q\Delta t$ is the number of erythrocytes lost over the period of time Δt. The Mean Value Theorem gives an average number of erythrocytes $m(\xi, v_F(\xi))$, for some $\xi \in (t, t + \Delta t)$, taken out in this time interval. A statement of balance can be written as:

$$Q\Delta t = W\Delta t\, m(\xi, v_F(\xi)) - [v_F(t + \Delta t) - v_F(t)]m(\xi, v_F(\xi)). \quad \text{(A.1)}$$

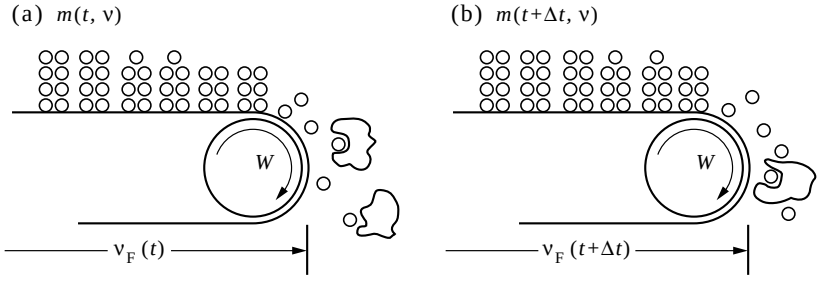

Fig. A1. Schematic illustration of the loss of mature erythrocytes to macrophages. The conveyor belt may have to stretch or shrink (an increase or decrease in the age of the mature erythrocytes) to maintain the assumed constant flux boundary condition corresponding to a fixed number of erythrocytes being destroyed.

The first term on the r.h.s. of (A.1) represents the number of mature cells lost because of the movement of the conveyor belt, while the second term represents either ones that stay on the belt due to a stretching or additional ones lost due to contraction. Dividing each side of (A.1) by Δt and taking the limit as $\Delta t \to 0$, the boundary condition becomes

$$Q = [W - \dot{v}_F(t)]m(t, v_F(t)).$$

This is the constant flux boundary condition required for the formation of the model, in Section 2.

APPENDIX B

Solutions from the Method of Characteristics

The method of characteristics is used to find the general solution of the partial differential equations and their boundary conditions given by eqns (1–5). A characteristic curve C_0 emanating from the origin in the (t, μ)-plane with $t > 0$ and $0 < \mu < \mu_F$ separates the (t, μ)-space into two regions, R_1 and R_2. This characteristic curve C_0 satisfies

$$t(s) = s \quad \text{and} \quad \mu(s) = \int_0^s V(E(\sigma))\,\mathrm{d}\sigma, \quad s \in [0, s_F],$$

where s_F is the *threshold value* implicity defined by

$$\mu_F = \int_0^{s_F} V(E(\sigma))\,\mathrm{d}\sigma.$$

The region R_1 provides solutions that depend on the initial conditions, while R_2 depends on the boundary conditions and provides the longer time solutions.

Given the pair of variables $(t, \mu) \in R_2$, a state-dependent delay, τ, is implicitly defined by (9). This delay represents the time required for the maturation level to go from 0 to μ and is found with knowledge of the history of the hormone concentration, E.

If the age-structure of the population satisfies the following initial conditions:

$$p(0, \mu) = \phi(\mu),$$
$$m(0, v) = \psi(v),$$

then the method of characteristics gives the following solution to the partial differential equation (2):

$$p(t, \mu) = \begin{cases} \phi\left(\mu - \int_0^t V(E(r))\,\mathrm{d}r\right) \exp\left[\int_0^t F\left(\mu - \int_w^t V(E(r))\,\mathrm{d}r, E(w)\right)\mathrm{d}w\right], \\ \qquad (t, \mu) \in R_1 \\ \dfrac{S_0(E(t-\tau))}{V(E(t-\tau))} \exp\left[\int_{t-\tau}^t F\left(\int_{t-\tau}^{\omega} V(E(r))\,\mathrm{d}r, E(w)\right)\mathrm{d}w\right], \\ \qquad (t, \mu) \in R_2 \end{cases} \tag{B.1}$$

where $F(\mu, E) = V(E)[\beta(\mu, E) - \alpha(\mu, E) - H(\mu)]$, and τ is determined by the threshold eqn (9). The method of characteristics applied to (2.5) produces the following result for the mature cells:

$$m(t, v) = \begin{cases} \psi(v - Wt) \exp\left[-W\int_0^t (v + W(\sigma - t))\,\mathrm{d}\sigma\right], \\ \qquad t < v/W \\ \dfrac{1}{W}\displaystyle\int_0^{\mu_F} h(\mu - \bar{\mu}) p(t - \frac{v}{W}, \mu)\,\mathrm{d}\mu \exp\left[-W\int_0^{v/W} \gamma(W\sigma)\,\mathrm{d}\sigma\right], \\ \qquad t > v/W \end{cases} \tag{B.2}$$

Equations (B.1) and (B.2) include transient solutions for small times t and the general solution for large times. If we choose t sufficiently large and examine only the long term behavior of these equations, then $M(t)$ is found to satisfy:

$$M(t) = \frac{1}{W}\int_0^{v_F(t)} \int_0^{\mu_F} h(\mu - \bar{\mu}) p\left(t - \frac{v}{W}, \mu\right)\mathrm{d}\mu \exp\left[-W\int_0^{v/W} \gamma(W\sigma)\,\mathrm{d}\sigma\right]\mathrm{d}v. \tag{B.3}$$

From (B.1) with $(t, \mu) \in R_2$, the precursor population p depends only on the hormone level E. Equation (B.3) shows that M depends only on p, so it follows that M is a function of E. Thus, eqns (7) and (B.3) form a system of integro-differential equations or threshold-type delay equations with the state-dependent delay τ defined implicitly by (9).